JOURNAL OF CATALYSIS 90, 183–193 (1984)

Mechanism of Formation of C_2-Oxygenated Compounds from CO + H_2 Reaction over SiO_2-Supported Rh Catalysts

HIDEO ORITA, SHUICHI NAITO, AND KENZI TAMARU

Department of Chemistry, Faculty of Science, The University of Tokyo, Hongo, Bunkyo-ku, Tokyo 113, Japan

Received February 24, 1984; revised July 5, 1984

The mechanism of acetaldehyde and ethanol formation from the CO + H_2 reaction below atmospheric pressure has been investigated by combining infrared spectroscopic measurement and ^{13}CO and $C^{18}O$ isotopic tracer studies with reaction kinetics. The rates of acetaldehyde and ethanol formation are markedly dependent on the nature of metal precursors employed. The addition of sodium cations depresses the total catalytic activity, while the selectivity for ethanol is increased by the addition of manganese cations. From the behavior of surface species under reaction conditions, it is concluded that acetaldehyde is formed through the following two steps: (i) CO insertion into C_1 species which are reaction intermediates for not only hydrocarbons but also for the methyl group in acetaldehyde, and (ii) subsequent formation of acetate ions whose one oxygen atom is supplied from the support, finally producing acetaldehyde. Differences in ^{18}O distribution in acetaldehyde and ethanol during the $C^{18}O$ + H_2 reaction indicate that ethanol is not produced via direct hydrogenation of acetaldehyde.

INTRODUCTION

The hydrogenation of carbon monoxide over transition metal catalysts produces a variety of compounds such as hydrocarbons, alcohols, aldehydes, and acids. The mechanism of hydrocarbon formation has been investigated by many workers (*1–7*). These results strongly suggest that the surface carbon formed by the dissociation of CO is an intermediate for hydrocarbon formation, implying that metals which dissociate CO readily are good catalysts for hydrocarbon formation unless the surface carbon is bound too strongly.

On the other hand, the mechanism of oxygenated compound formation has not been elucidated so far. Only very recently, Takeuchi and Katzer (*8*) and Tamaru *et al.* (*9*) have demonstrated that methanol is produced via hydrogenation of nondissociative CO. Tamaru *et al.* (*10*) have reported that palladium catalysts prepared from M_2PdCl_4 (M = alkali metals) type complexes produce methanol selectively from the CO + H_2 reaction at atmospheric pressure; they also demonstrated the important role of sodium and lithium cations in the formation of active sites for methanol synthesis. Furthermore, Takeuchi and Katzer (*11*) have studied the mechanism of ethanol formation by using a 50–50 mixture of ^{13}CO and $C^{18}O$, and proposed a rather complicated mechanism involving CO insertion into adsorbed carbene species instead of a methyl radical followed by isotopic scrambling in the adsorbed intermediate. However, they did not differentiate between the two carbon atoms of ethanol, the methyl carbon, and the hydroxymethylene carbon, and they based their conclusions about the mechanism exclusively on the *parent* peaks of labeled ethanol in the mass spectra.

In the present study, the mechanism of acetaldehyde and ethanol formation has been studied through reaction kinetics, infrared spectra of adsorbed species, and the behavior of isotopic tracers. We could differentiate the carbon isotope distribution in the methyl group of acetaldehyde from that in the formyl group by observing the fragmentation pattern of mass spectra. The

0021-9517/84 $3.00

results indicate that acetaldehyde is produced via CO insertion into C_1 species, which are the intermediates for hydrocarbon formation. The nature of active sites for the formation of acetaldehyde and ethanol as well as hydrocarbons is discussed.

EXPERIMENTAL

Catalyst preparation and reactor. The catalysts were prepared by impregnating aqueous solutions of metal salts ($RhCl_3$, $Rh(NO_3)_3$, Na_3RhCl_6, $[Rh(NH_3)_6]Cl_3$, or a mixture of $RhCl_3$ and $MnCl_2$) onto SiO_2 (Aerosil). After impregnation, the catalysts (5 wt% Rh) were dried in air at 383 K for ca. 12 h. These materials were ground into a fine powder and put into a U-shaped glass reactor, which was connected to a closed gas recirculation system, and dried by air circulation at room temperature with a liquid nitrogen cold trap for ca. 15 h prior to the reduction by hydrogen at 473–723 K for several hours.

The hydrogenation of CO was carried out in the recirculation system with a liquid nitrogen cold trap, which made product analysis easy and prevented secondary reactions such as olefin hydrogenation and water–gas shift. The reaction products were analyzed and separated into each component by gas chromatography using molecular sieve 5A and Porapak Q columns. The isotope distribution in each of the separated products was determined by a quadrupole mass filter (UTI 100C). In order to make the mass analyses of hydrocarbons easier, separated hydrocarbons were oxidized with O_2 gas to CO_2 over Pd black (Nippon Engelhard) at 573 K, and the carbon isotope distribution in the CO_2 was measured.

Hydrogen gas was purified by passing it through an Engelhard Deoxo unit followed by a liquid nitrogen cold trap. Deuterium (Showa Denko) and ^{12}CO (Takachiho Kagaku) were passed through a liquid nitrogen cold trap before use. Isotope-labeled carbon monoxide (^{13}CO, 90% purity; $C^{18}O$, 99% purity) was purchased from Proc and used without further purification. A aldehyde was obtained from Merck and rified by outgassing and vacuum distilla from a dry ice–methanol cold trap to a uid nitrogen cold trap.

Infrared spectroscopy. The catal were pressed into self-supporting disk cm in diameter and 40–50 mg in weigh ca. 150 atm. One or two disks were pl in an infrared cell, which was connecte a closed gas circulation system, and tre under various atmospheres inside the c

Infrared spectra were measured at r temperature by a JEOL JIR-03F Fou transform infrared spectrometer with MCT (HgTe-CdTe) detector cooled by uid nitrogen. Spectral resolution of the IR spectrometer was fixed at 2 cm^{-1} in region 4000–1000 cm^{-1}.

RESULTS AND DISCUSSION

Reaction Kinetics and Product Distributions

The catalytic properties of the var rhodium catalysts in the CO + H_2 reac at 453 K were investigated by chan metal precursors. The results are show Table 1. The activity and selectivity o rhodium catalysts showed a large differ depending on metal precursors. Only small amounts of methanol (selectivit 0.2%) were produced over all the cata investigated. Figure 1 shows a typical drocarbon distribution of the CO + H_2 r tion in a Schulz–Flory plot. The hydr bon distribution obeyed the Schulz–F equation from C_3 to C_7. The dispersion the selectivity for C_2-oxygenated c pounds of all the catalysts (except the prepared from $[Rh(NH_3)_6]Cl_3$) were tively high. The most active catalyst fo formation of acetaldehyde was $RhCl_3/S$ but the most selective catalyst $Rh(NO_3)_3/SiO_2$. The activity of the l catalyst was only one-thirtieth of that o former. As the reaction temperature creased from 453 to 393 K, the select

TABLE 1

$CO + H_2$ Reaction over Various Rhodium Catalysts Supported on SiO_2

Metal precursors	H/Rh[a] (%)	Rate of CO consumption[b] (ml-STP/h · g-cat.)	Selectivity[c] (%)	
			MeCHO	EtOH
$RhCl_3$	52	13.8	12	0.4
$RhCl_3 + MnCl_2$[d]	32	4.6	18	11
Na_3RhCl_6	40	0.08	32	—
$[Rh(NH_3)_6]Cl_3$	2	0.72	2	0.1
$Rh(NO_3)_3$	61	0.14	40	1

[a] Based on H_2 adsorption at room temperature after H_2 reduction at 573 K.
[b] Reaction condition, $T = 453$ K, $P^\circ = 270$ Torr (1 Torr = 133.3 Pa), $H_2/CO = 2$.
[c] Calculated by carbon efficiency.
[d] Mn/Rh = 1.5.

for the acetaldehyde formation over $RhCl_3/SiO_2$ increased up to 35% and the rate of CO consumption decreased to 0.3 ml-STP/h · g-cat., which is about twice the value for $Rh(NO_3)_3/SiO_2$ at 453 K. These results suggest that chlorine which remains in the catalysts after hydrogen reduction at high temperature plays an important role for the enhancement of catalytic activity of rhodium metal. On the other hand, the catalyst prepared from $[Rh(NH_3)_6]Cl_3$ showed the lowest dispersion and selectivity for C_2-oxygenated compounds, suggesting that well dispersed rhodium is effective for the formation of C_2-oxygenated compounds. Addition of sodium cations decreased the rate of CO consumption drastically, but increased the selectivity for C_2-oxygenated compounds. The effect of doping alkali metal cations on SiO_2-supported rhodium catalysts is very different from that on TiO_2-supported rhodium catalysts as reported previously (*12*). That is, in the case of non-doped $RhCl_3/TiO_2$ or $(NH_4)_3RhCl_6/TiO_2$ catalyst C_2-oxygenated compounds were not produced by the $CO + H_2$ reaction but the addition of alkali metal cations to these catalysts increased the rate as well as the selectivity of C_2-oxygenated compound formation. This difference may be due to the metal–support interaction.

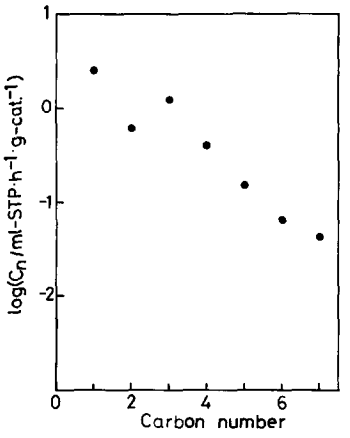

FIG. 1. Typical hydrocarbon distribution of the CO + H_2 reaction in a Schulz–Flory plot ($RhCl_3/SiO_2$ catalyst, $T = 453$ K, $P^\circ = 270$ Torr, $H_2/CO = 2$).

The addition of manganese cations to rhodium catalysts is believed to enhance the rate of C_2-oxygenated compound formation without changing the selectivity (*13*), but it was effective for improving the selectivity for ethanol formation in this study. This discrepancy is probably due to the different amount of added manganese to rhodium (Mn/Rh = 1.5 in this study and 0.04 in Ref. *13*).

The dependences of product formation rate on the pressures of hydrogen and carbon monoxide were examined, and the results for Na_3RhCl_6/SiO_2 catalyst are

TABLE 2

Dependence of Product Formation on Pressure of Hydrogen and Carbon Monoxide over Na_3RhCl_6/SiO_2 at 473 K[a,b]

Products	X	Y
CH_4	0.9	−0.8
MeCHO	0.9	0

[a] The values X and Y were determined from the initial rate of CO + H_2 reaction, by changing the partial pressure of H_2 ($P(CO)$ = 90 Torr constant) and the partial pressure of CO ($P(H_2)$ = 180 Torr constant), respectively.

[b] Rate $\alpha P(H_2)^X \cdot P(CO)^Y$.

shown in Table 2. The formation rates of methane and acetaldehyde exhibited the same pressure dependence upon the partial pressure of hydrogen. As the partial pressure of carbon monoxide was increased, the rate of methane formation was depressed but that of acetaldehyde was unchanged. This result suggests that the mechanism of acetaldehyde formation is different from that of methane.

Activation energies of product formation from the CO + H_2 reaction over $RhCl_3/SiO_2$ and Na_3RhCl_6/SiO_2 are summarized in Table 3. Addition of sodium cations increased the activation energies of all the products corresponding to a decrease of the catalytic activity.

TABLE 3

Activation Energies of Product Formation from CO + H_2 Reaction over $RhCl_3/SiO_2$ and Na_3RhCl_6/SiO_2 (P^o = 270 Torr, H_2/CO = 2)

Catalysts	Activation energies/kcal mol^{-1}			
	CH_4	C_2^+[a]	MeCHO	CO_2
$RhCl_3/SiO_2$[b]	20	19	16	15
Na_3RhCl_6/SiO_2[c]	23	21	21	23

[a] Hydrocarbons higher than methane.

[b] T = 393–473 K.

[c] T = 433–523 K.

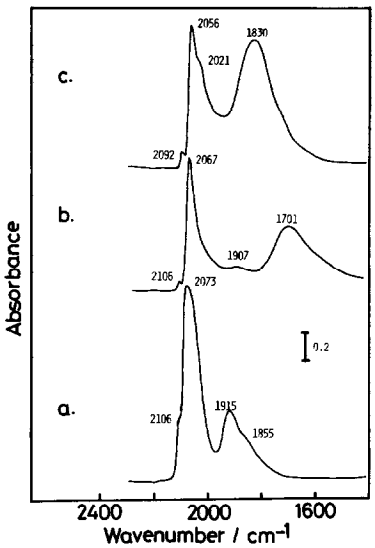

FIG. 2. Infrared spectra of CO adsorbed on rhodium catalysts (T = 300 K, P_{CO} = 8 Torr): (a) $RhCl_3/SiO_2$; (b) $RhCl_3$ + $MnCl_2/SiO_2$ (Mn/Rh = 1.5); (c) Na_3RhCl_6/SiO_2.

Infrared Spectra of Adsorbed Species

Difference in the catalytic activities of various catalysts shown in Table 1 was investigated with Fourier transform infrared spectroscopy. Carbon monoxide adsorption on supported rhodium catalysts has been extensively studied by a number of workers (*14–21*), and three types of chemisorbed CO are reported on the surface of supported rhodium catalyst at ca. 300 K. Twin species are considered to be adsorbed on partially oxidized Rh sites (*15, 16, 19–22*), while linear and bridge species are adsorbed on Rh^0 sites. Infrared spectra of adsorbed CO on three typical catalysts at room temperature are shown in Fig. 2. Although three types of chemisorbed CO were observed for all the catalysts, the intensity of the twin species was very weak and appeared only as a shoulder of strong bands of linear species. The addition of sodium or manganese cations reduced the band intensity of the linear species, increased that of the bridge species, and caused the CO(a) band to shift to lower wave numbers. These observations mean

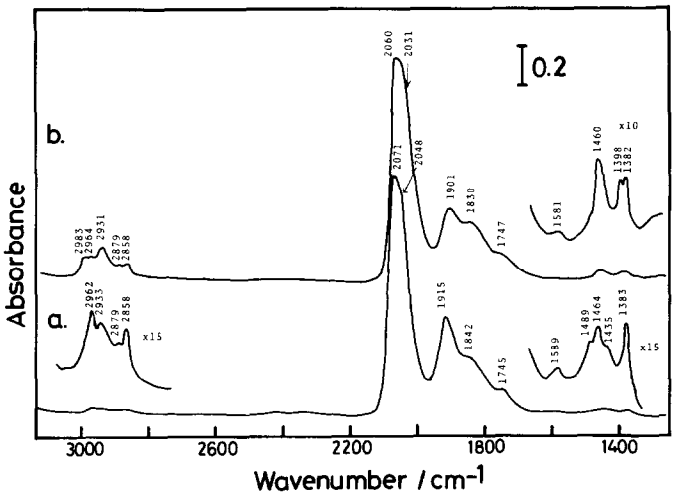

FIG. 3. Infrared spectra of adsorbed species on $RhCl_3/SiO_2$ catalyst: (a) CO + H_2 reaction at 453 K for 1 h (P° = 250 Torr, CO/H_2 = 2); (b) decomposition of acetaldehyde at 453 K for 1.5 h (P = 5 Torr).

that the electronic state of rhodium metal is modified by doping with sodium or manganese cations. The band intensity of bridge species correlated well with the catalytic activity; the catalytic activity decreased as the intensity of bridge species of chemisorbed CO increased.

Figures 3–5 show the infrared spectra of adsorbed species both during the CO + H_2 reaction and after the decomposition of acetaldehyde over three typical catalysts ($RhCl_3/SiO_2$, Na_3RhCl_6/SiO_2, and $RhCl_3$ + $MnCl_2/SiO_2$). The spectra during the CO + H_2 reaction are very similar to those after the decomposition of acetaldehyde except that the wave number of CO(a) is shifted to lower values after the decomposition of acetaldehyde and two strong bands at 1577 and 1425 cm^{-1} appear for Na_3RhCl_6/SiO_2. These results indicate that the decomposition of acetaldehyde occurs very easily and produces surface species similar to those

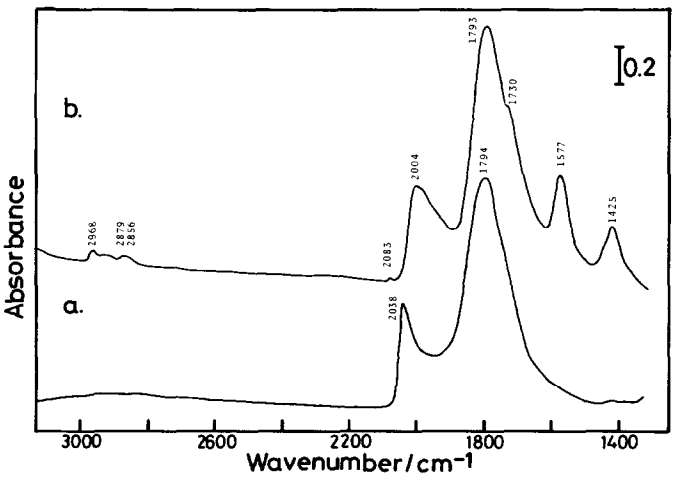

FIG. 4. Infrared spectra of adsorbed species on Na_3RhCl_6/SiO_2 catalyst. (a) CO + H_2 reaction at 453 K for 12.5 h (P° = 170 Torr, H_2/CO = 2); (b) decomposition of acetaldehyde at 453 K for 1.5 h (P = 5 Torr).

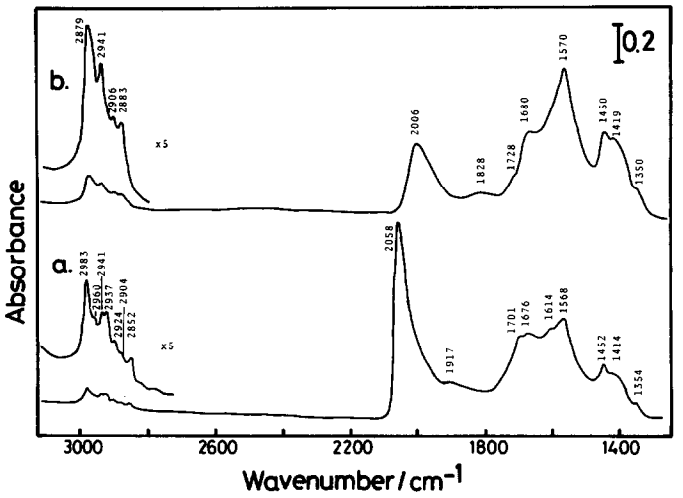

FIG. 5. Infrared spectra of adsorbed species on $RhCl_3$ + $MnCl_2/SiO_2$ catalyst (Mn/Rh = 1.5): (a) CO + H_2 reaction at 523 K for 1 h (P° = 250 Torr, CO/H_2 = 2); (b) decomposition of acetaldehyde at 473 K for 0.5 h (P = 5 Torr).

during the CO + H_2 reaction. The shift of CO(a) after the decomposition of acetaldehyde to the lower wave number may be due to the lower coverage of CO(a) (*14, 17, 18*). The two strong bands at 1577 and 1425 cm^{-1} for Na_3RhCl_6/SiO_2 can be assigned to the asymmetric and symmetric modes of O–C–O stretching vibration of adsorbed acetate ions (*23*) stabilized by the presence of sodium cations. The formation of acetate ion from ethanol over alumina (*24*) and from acetaldehyde over Ni/SiO_2 (*25*) has been reported previously and is in good agreement with this work. To confirm this assignment, the adsorption of acetic acid (P < 1 Torr) was carried out at room temperature. A pair of strong bands was observed at 1568 and 1417 cm^{-1}, which agrees well with the results of the acetaldehyde adsorption. Another band at 1720 cm^{-1} was observed when the adsorption of acetic acid was examined at pressures higher than 10 Torr; this may be attributed to the CO stretching vibration of chemisorbed surface ester groups, $CH_3\overset{\overset{O}{\|}}{C}OSi$, formed by the reaction of the acid and surface hydroxyl groups (*26*). After the CO + H_2 reaction for 12.5 h over $NaRhCl_6/SiO_2$, the acetate ion bands could not be observed, maybe because of the slow rate of the acetaldehyde formation. Over $RhCl_3/SiO_2$, which is the most active catalyst for the formation of acetaldehyde, the decomposition of acetaldehyde occurred very fast even at room temperature. Also, the intensities of CO(a) bands were almost the same as those during the CO + H_2 reaction, but the bands of acetate ion were not observed clearly in this case because of the low stability of acetate ion on rhodium metal. A more detailed assignment was carried out by labeling the adsorbed species with stable isotope and is discussed in the following section.

In the case of the manganese doped catalyst the bands observed at 1568 and 1414 cm^{-1} can be assigned to the asymmetric and symmetric modes of O–C–O stretching vibration of adsorbed acetate ion by the analogy of the band position and intensity with the spectra for Na_3RhCl_6/SiO_2. The shape of the bands at around 3000–2800 cm^{-1} after the decomposition of acetaldehyde is very similar to those obtained by the adsorption of acetaldehyde on Ni/SiO_2 at room temperature (*25*), and are attributed to CH_3CH_2OSi or the diadsorbed alkoxide

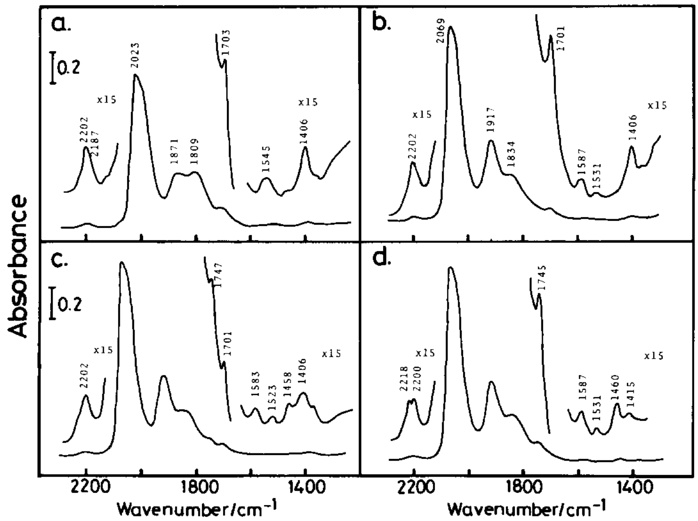

FIG. 6. Infrared spectra of isotopically labeled species adsorbed on $RhCl_3/SiO_2$ catalyst: (a) $^{13}CO + D_2$ reaction at 453 K for 3 h; (b) ^{12}CO adsorption at room temperature after (a); (c) $^{12}CO + D_2$ reaction at 453 K for 0.5 h after (b); (d) $^{12}CO + D_2$ reaction at 453 K for 3.75 h after (b) (P° = 230 Torr, CO/D_2 = 2).

$CH_3CH{-}O$ (with both C and O bonded to M). During the $CO + H_2$ reaction, weak bands at 2960, 2924, and 2852 cm^{-1} were observed in addition to the bands observed after the decomposition of acetaldehyde. The bands at 2960 and 2924 cm^{-1} are assigned to the asymmetric C–H stretching vibrational modes of methyl and methylene groups of adsorbed hydrocarbon species, respectively, and the band at 2852 cm^{-1} is assigned to the symmetric C–H stretching vibrational mode of methylene groups.

The results of the infrared spectroscopic measurements suggest that the adsorbed acetate ions might play an important role during the $CO + H_2$ reaction. Therefore, the dynamic behavior of adsorbed species during the $CO + H_2$ reaction was investigated by isotopic tracer methods.

Dynamic Behavior of Adsorbed Species during Reaction

Figure 6 shows the infrared spectra of isotopically labeled species adsorbed on $RhCl_3/SiO_2$ catalyst during the $^{13}CO + D_2$ reaction followed by the replacement of $^{13}CO + D_2$ with $^{12}CO + D_2$, which results in replacement of adsorbed ^{13}CO with ^{12}CO. Deuterium was used instead of hydrogen in order to avoid the overlap of absorption bands in the region 1500–1300 cm^{-1}. After the $^{13}CO + D_2$ reaction at 453 K for 3 h (Fig. 6a), strong bands at 2023, 1871, and 1809 cm^{-1} were observed and can be assigned to the linear and bridged forms of $^{13}CO(a)$. Weak bands located at 2202, 1703, 1545, and 1406 cm^{-1} were also observed. After the short evacuation at room temperature, ^{12}CO was introduced onto the catalyst. Three CO(a) bands were shifted rapidly to 2069, 1917, and 1834 cm^{-1}, which indicates a rapid exchange of adsorbed ^{13}CO with ^{12}CO in the gas phase. A weak band at 1545 cm^{-1} was also shifted to 1587 cm^{-1}. However, this band did not appear unless the mixture of CO and H_2 (or D_2) was introduced onto the catalyst at the reaction temperature, suggesting that this band is due to some hydrogenated species of CO. This band disappeared easily on evacuation at 373 K or hydrogen reduction below 453 K, showing its high reactivity; its band position was very similar to that of formyl

group coordinated to some transition metal complexes (1610–1555 cm^{-1}) (*27–31*). The exact assignment of this species could not be done because the corresponding C–H (or C–D) stretching vibration was not observed owing to the small extinction coefficient of the C–H (or C–D) stretching vibration. Figures 6c and d show the dynamic behavior of adsorbed species during the $^{12}CO + D_2$ reaction at 453 K subsequent to the $^{13}CO + D_2$ reaction. As the reaction proceeded, the bands at 2202, 1701, and 1406 cm^{-1} decreased and the new bands at 2218, 1745, and 1460 cm^{-1} appeared, indicating that adsorbed species composed of ^{13}C were converted to those of ^{12}C. In comparison with the infrared spectrum during the $^{12}CO + H_2$ reaction in Fig. 3, the band at 2202 cm^{-1} and a shoulder at 2187 cm^{-1} can be assigned to the asymmetric ^{13}C–D stretching vibration of methyl group of adsorbed hydrocarbons and that of methylene group, respectively, which were shifted to the higher wave numbers during the $^{12}CO + D_2$ reaction. The value of this isotope shift (ca. 16 cm^{-1}) is reasonable when the conversion of $^{13}CD_3$ group into $^{12}CD_3$ group is considered. The intensity of the bands of adsorbed hydrocarbon species was decreased on evacuation at 453 K, but increased again to some extent during the hydrogenation at 373 K. The same phenomenon was observed previously for Ru/SiO_2 (*32*), which was explained by the dehydrogenation of adsorbed hydrocarbon species by evacuation and its reverse reaction by hydrogenation on a limited part of Ru surface. Therefore, it can be considered that the adsorbed hydrocarbon species observed in this study is also adsorbed on a part of Rh metal. The band at 1745 (1701) cm^{-1} can be assigned to the ^{12}CO (^{13}CO) stretching vibration of adsorbed acetyl species through the comparison with the band position of acetyl species in the literature (*33–35*). This acetyl species was the most stable toward evacuation or hydrogenation at 453 K among all the adsorbed species including CO(a) observed by infrared spectroscopy, suggesting that it is not adsorbed on Rh metal but on the support near Rh particles.

As can be seen in Fig. 6, the adsorbed hydrocarbon and acetyl species behaved like reaction intermediates. However, the real contribution of these species to the overall reaction cannot be determined unless the rate at which the adsorbed species are converted to the products is compared with the overall rate of product formation. For this comparison, it is indispensable to know the extinction coefficients of adsorbed species, which is quite difficult to measure in this study. Accordingly, volumetric experiments by using isotopes over a large amount of catalyst were carried out. The isotope distribution in products was measured with the aid of a quadrupole mass filter in order to determine the real contribution of adsorbed species to the overall reaction quantitatively. The experimental procedure was as follows: (i) the $^{13}CO + H_2$ reaction was carried out at 393 K for 3.5 h over freshly reduced $RhCl_3SiO_2$, and surface species as shown in Fig. 6a were accumulated on the catalyst; (ii) the catalyst was cooled to room temperature and a sufficient amount of ^{12}CO was introduced to replace the molecularly adsorbed ^{13}CO; (iii) a $^{12}CO + H_2$ mixture was introduced and the catalyst was heated to 393 K as rapidly as possi-

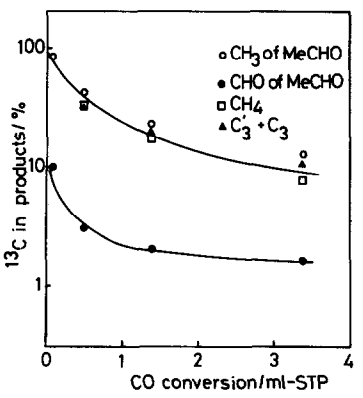

FIG. 7. Carbon isotope distribution in products during $^{12}CO + H_2$ reaction at 393 K over $RhCl_3/SiO_2$ catalyst after $^{13}CO + H_2$ reaction at 393 K for 3.5 h (P° = 240 Torr, H_2/CO = 1, ^{13}CO 90%, 3.1 g catalyst).

ble; (iv) the ^{13}C distribution in products was analyzed with time. As shown in Fig. 7, the ^{13}C distribution in methyl group of acetaldehyde exhibited almost the same behavior as those of hydrocarbons and could be extrapolated to the purity of used ^{13}CO (90%) at the initial stage of reaction. The hydrocarbons higher than methane were represented by C_3 hydrocarbons which was the most abundant product. Occasionally, ^{13}C distributions in C_2 or C_4 hydrocarbons were measured and similar values to that of C_3 hydrocarbons were obtained. On the other hand, the ^{13}C distribution in formyl group of acetaldehyde was markedly different from those of hydrocarbons, and decreased rapidly to the natural abundance of ^{13}C (1.1%). This fact indicates that during the steady state CO + H_2 reaction, there exist common C_1 intermediates through which hydrocarbons and methyl group of acetaldehyde are formed, and acetaldehyde is produced via CO insertion into these C_1 intermediates. From the fact that the initial ^{13}C distribution in the formyl group of acetaldehyde is ca. 10%, it is deduced from infrared spectroscopy that the conversion rate of the acetyl species to acetaldehyde is only 10% of the overall rate of acetaldehyde formation and that the contribution of this acetyl species to the overall reaction is small.

Similar behavior of the ^{13}C distribution in hydrocarbons during $^{12}CO + H_2$ reaction after the accumulation of ^{13}C surface hydrocarbons species was previously observed for Ru/SiO_2 (*5*), and it was concluded from the reactivity of deposited carbon that *all* the hydrocarbon products are produced via dissociatively adsorbed CO with no CO insertion. In the present study, the reactivity of deposited carbon formed by the Boudouard reaction was also studied by the use of ^{13}CO. However, only a very small amount of deposited carbon was formed on $RhCl_3/SiO_2$ ($\theta_c = 0.025$, $T = 473$ K, $t = 3$ h). The initial ^{13}C distribution in the hydrocarbons during the $^{12}CO + H_2$ reaction was only 30%, and an induction period of acetaldehyde formation was observed. These

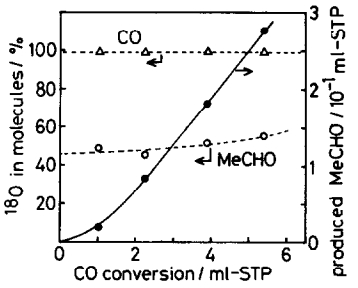

FIG. 8. Oxygen isotope distribution during $C^{18}O + H_2$ reaction at 423 K over $RhCl_3/SiO_2$ catalyst (P° = 170 Torr, $H_2/CO = 2$, $C^{18}O$ 99%, 0.7 g catalyst).

results indicate that the dissociation of CO on Rh in the absence of hydrogen is very slow, and that the carbon deposited on Rh is not so reactive as that on Ru (*5*) and inhibits acetaldehyde formation. The real contribution of carbon deposited on Rh under the steady state reaction could not be completely understood from the results of this work.

In order to study the nature of the active site for the acetaldehyde formation, the reaction of $C^{18}O$ and hydrogen was carried out at 423 K over freshly reduced $RhCl_3/SiO_2$, and the ^{18}O distribution in the reactant and products was measured. The results are shown in Fig. 8. During the reaction, the ^{18}O distribution in CO was constant at 99%, but that in acetaldehyde was nearly 50% at the initial stage of the reaction and gradually increased. These results suggest that the reaction intermediates which form acetaldehyde via CO insertion into C_1 species have a structure like acetate

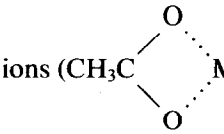

ions (CH_3C M) with one oxygen atom being supplied by CO and the other by the support. These intermediates are hydrogenated rapidly to acetaldehyde before further exchange of oxygen with the support takes place (i.e., the residence time of this species on the catalyst is very small). The acetate ions adsorbed on $RhCl_3/SiO_2$ could not be detected by infrared spectroscopy (see

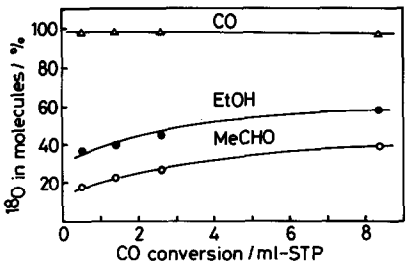

FIG. 9. Oxygen isotope distribution during $C^{18}O$ + H_2 reaction at 423 K over $RhCl_3$ + $MnCl_2/SiO_2$ catalyst (P^o = 170 Torr, H_2/CO = 2, $C^{18}O$ 99%, 1.0 g catalyst).

Figs. 3 and 6), but this result can be explained by considering that the residence time of acetate species and the number of active sites for the formation of acetaldehyde are very small.

For the manganese cation doped catalyst, the activity was one third of that for $RhCl_3/SiO_2$. However, the acetate ions adsorbed on the catalyst under reaction conditions were observed by infrared spectroscopy, and the selectivity for ethanol formation was increased. In order to compare the formation mechanism of acetaldehyde with that of ethanol, the reaction of $C^{18}O$ + H_2 was carried out and the results are shown in Fig. 9. The ^{18}O distribution in the acetaldehyde was decreased to <20%, which suggests that manganese cations stabilize the acetate intermediates as sodium cations do the formate ions for palladium catalysts (*10*); the manganese cations also promote oxygen exchange with the support. The difference in the ^{18}O distributions in acetaldehyde and ethanol indicates that ethanol is not produced via direct hydrogenation of acetaldehyde. In fact, the addition of acetaldehyde to the CO + H_2 reaction under steady state conditions did not increase the formation rate of ethanol, but decomposition of acetaldehyde occurred. From these observations, it is concluded that the active sites for the formation of C_2-oxygenated compounds are located near the contact points between the rhodium metal and the support, as was similarly concluded in the case of supported palladium catalysts (*10*).

REFERENCES

1. Wentrcek, P. R., Wood, B. J., and Wise, H., *J. Catal.* **43,** 363 (1976).
2. Araki, M., and Ponec, V., *J. Catal.* **44,** 439 (1976).
3. Sachtler, J. W. A., Kool, J. M., and Ponec, V., *J. Catal.* **56,** 284 (1979).
4. Biloen, P., Helle, J. N., and Sachtler, W. M. H., *J. Catal.* **58,** 95 (1979).
5. Kobori, Y., Yamasaki, H., Naito, S., Onishi, T., and Tamaru, K., *J. Chem. Soc., Faraday Trans. I* **78,** 1473 (1982).
6. Cant, N. W., and Bell, A. T., *J. Catal.* **73,** 257 (1982).
7. Biloen, P., Helle, J. N., van den Berg, F. G. A., and Sachter, W. M. H., *J. Catal.* **81,** 450 (1983).
8. Takeuchi, A., and Katzer, J. R., *J. Phys. Chem.* **85,** 937 (1981).
9. Kobori, Y., Yamasaki, H., Naito, S., Onishi, T., and Tamaru, K., *Chem. Lett.* 553 (1983).
10. Kikuzono, Y., Kagami, S., Naito, S., Onishi, T., and Tamaru, K., *Chem. Lett.* 1249 (1981); *Faraday Discuss. Chem. Soc.* **72,** 135 (1981).
11. Takeuchi, A., and Katzer, J. R., *J. Phys. Chem.* **86,** 2438 (1982).
12. Orita, H., Naito, S., and Tamaru, K., *Chem. Lett.* 1161 (1983).
13. Wilson, T. P., Kasai, P. H., and Ellgen, P. C., *J. Catal.* **69,** 193 (1981).
14. Yang, A. C., and Garland, C. W., *J. Phys. Chem.* **61,** 1504 (1957).
15. Primet, M., *J. Chem. Soc., Faraday Trans. I* **74,** 2570 (1978).
16. Knözinger, H., Thornton, E. W., and Wolf, M., *J. Chem. Soc., Faraday Trans. I* **75,** 1888 (1979).
17. Yates, D. J. C., Murrell, L. L., and Prestridge, E. B., *J. Catal.* **57,** 41 (1979).
18. Yates, J. T., Duncan, T. M., Worley, S. D., and Vaughan, R. W., *J. Chem. Phys.* **70,** 1219 (1979); **70,** 1225 (1979).
19. Yates, J. T., Duncan, T. M., and Vaughan, R. W., *J. Chem. Phys.* **71,** 3908 (1979).
20. Cavanagh, R. R., and Yates, J. T., *J. Chem. Phys.* **74,** 4150 (1981).
21. Rice, C. A., Worley, S. D., Curtis, C. W., Guin, J. A., and Tarrer, A. R., *J. Chem. Phys.* **74,** 6487 (1981).
22. Yates, J. T., and Kolansinski, K., *J. Chem. Phys.* **79,** 1026 (1983).
23. Ito, K., and Bernstein, H. J., *Canad. J. Chem.* **34,** 170 (1956).
24. Greenler, R. G., *J. Chem. Phys.* **37,** 2094 (1962).
25. Young, R. P., and Sheppard, N., *J. Catal.* **20,** 340 (1971).
26. Young, R. P., *Canad. J. Chem.* **47,** 2237 (1969).

27. Collins, T. J., and Roper, W. R., *J. Chem. Soc., Chem. Commun.* 1044 (1976).
28. Gladyz, J. A., and Selover, J. C., *Tetrahedron Lett.* **4,** 319 (1978).
29. Pruett, R. L., Schoening, R. C., Vidal, J. L., and Fiato, R. A., *J. Organomet. Chem.* **182,** C57 (1979).
30. Collman, J. P., and Winter, S. R., *J. Amer. Chem. Soc.* **95,** 4089 (1973).
31. Casey, C. P., and Neumann, S. M., *J. Amer. Chem. Soc.* **98,** 5395 (1976).
32. Yamasaki, H., Kobori, Y., Naito, S. Onishi, T., and Tamaru, K., *J. Chem. Soc., Faraday Trans. I* **77,** 2913 (1981).
33. Baird, M. C., Mague, J. T., Osborn, J. A., and Wilkinson, G., *J. Chem. Soc.* (*A*) 1347 (1967).
34. Eggleston, D. L., Baird, M. C., Lock, C. J. L., and Turner, G., *J. Chem. Soc., Dalton* 1576 (1977).
35. Primet, M., and Garbowski, E., *Chem. Phys. Lett.* **72,** 472 (1980).